Coupling Analysis and Feedforward Compensation Design of Two-axis Gimbal Controller

1st Mengchen Cai
College of Electrical Engineering
Sichuan University
Chengdu, China
mchencai@163.com

2nd Tao Zhao*
College of Electrical Engineering
Sichuan University
Chengdu, China
zhaotaozhaogang@126.com
*Corresponding author

***Abstract*—Gimbal systems are pivotal in fields ranging from aerospace to photography, demanding high precision and stability. Traditional pitch-yaw decoupled control strategies ignores the dynamics coupling of the two axes, thus often faltering to meet the stringent requirements for precision and stability. This research dissects the intricate coupling effects between the gimbal axes. By implementing a strategic feedforward compensation channel, the system is reduced to two decoupled double-integrator with minor disturbance terms and further stabilized by two cascade PID controllers. The hidden state used by the compensation term is acquire by our designed Luenberger observer, whose stability is proved to guarantee the correctness of our algorithm. Simulations based on real-world parameters validates the performance of our proposed algorithm and superiority than pure PID. Our methodology not only stabilizes the gimbal with reduced tracking error and quicker response times but also offers a robust framework adaptable to other multi-axis control systems.**

***Index Terms*—gimbal controller, dynamic compensation, feedforward control, PID**

I. Introduction

Gimbal systems, renowned for their versatility and utility, have found extensive applications across various domains, from aerospace [1] and robotics to cinematography and surveillance [2–4]. The significance of research in this area lies in its potential to enhance the precision and stability of these systems, enabling them to meet the demands of intricate tasks in today's technologically advanced world.

Control strategies for gimbal systems have traversed a multifaceted research landscape, focusing on achieving superior performance and robustness. Among the prominent research paths, feed-forward dynamic compensation control and cascade PID control have emerged as pivotal techniques, offering promising solutions to the challenges posed by these systems' inherent complexities and high real-time response demand.

Numerous scholars have contributed various methodologies for implementing feedforward compensation in pursuit of enhancing the precision of gimbal control. Martin and Zdeněk [5] explored a feedforward compensation approach leveraging linear acceleration. Similarly, Mu [6] introduced a feed-forward compensation scheme that incorporates linear acceleration. Han et al. [7] advanced the field by proposing an adaptive feedforward method, which considers angular rate and acceleration rate and relies on a simplified FxLMS (Filtered-x Least Mean Square) algorithm. In a distinctive endeavor, Zheng et al. [8] devised a modified current integral feed-forward (CIF) control scheme, primarily aimed at enhancing the dynamic response of the system. Further enhancing the precision of feedforward compensation, Cui and Yan [9] pursued a unique approach by precisely determining the equivalent torque responsible for mitigating rotor disturbances in the gimbal system. These works collectively constitute a rich landscape of research, contributing significantly to the development of feed-forward compensation strategies for gimbal control.

Our research embarks on a distinctive path. We begin by modeling the gimbal system as a non-linear entity based on rigid body mechanics and frictionless assumption, a crucial step to capture its intricate dynamics accurately. Our analysis delves into the intricate interplay between pitch and yaw angles, recognizing the coupling effects that often demand sophisticated control strategies. To address these challenges, our approach employs feed-forward dynamic compensation to guide the system towards a working point approximating a simple double integrator system. However, the exact of the system yaw and pitch angles and their time derivative may not be measured directly or accurate enough due to the hardware constraints. We designed state observers to track the state and filter the noise. Subsequently, we implement a cascade control system, meticulously designed to govern the system with precision and agility.

In the forthcoming sections of this paper, we delve deeper into the theoretical foundations, algorithmic intricacies, and experimental validations of our novel control scheme for the two-axis gimbal system. Section II introduces our definition of system coordinates and analyze the system dynamics. Section III proposed our detailed control scheme design. Section IV provides simulation results based on real world system parameters. Section V finally concludes the paper.

II. Modeling of Two-axis Gimbal

The common two-axis gimbal platforms generally have three types of structural designs: polar-axis, horizontal-axis, and azimuth-axis. The system object studied in this article is an azimuth-axis gimbal. In this section, we provide an accurate description of the system dynamics from the system control

input and the current applied on two motors, to the yaw and pitch angle behavior [10]. The dynamics mathematical model is the basis of our further design of control scheme. We observe that, due to the mechanics coupling, the torque from pitch motor also influence the yaw dynamics and vice versa. This coupling raise challenges on the design of control algorithm to perform fast, stable and accurate angle tracking, and is the motivation of our design of non-linear feed-forward compensation.

A. Reference frame and coordinates

The mathematical model of a gimbal is derived from the mechanical structure and rotational process of the gimbal, which includes the corresponding kinetic and dynamic equations.

We first define the system coordinates and frames and then introduce the system dynamics based on defined coordinate systems. The inertial frame is denote by $\mathcal{F}$, which is fixed on the ground. Since the gimbal system is installed on a vehicle (ground, aerial, underwater, etc.) which is usually not inertial frame, we denote the body frame as $\mathcal{B}$ as shown in Fig. 1, which is fixed on body base. Connected by the yaw axis with the body base, we denote the yaw frame as $\mathcal{Y}$. Finally, the pointing frame is connected on the yaw frame by the pitch axis, and is denoted by $\mathcal{P}$. Functional devices such as cameras are usually installed on the pointing system. Define the yaw angle and angular velocity of the gimbal as $\psi, \dot{\psi}$ and the pitch angle and angular velocity as $\beta, \dot{\beta}$.

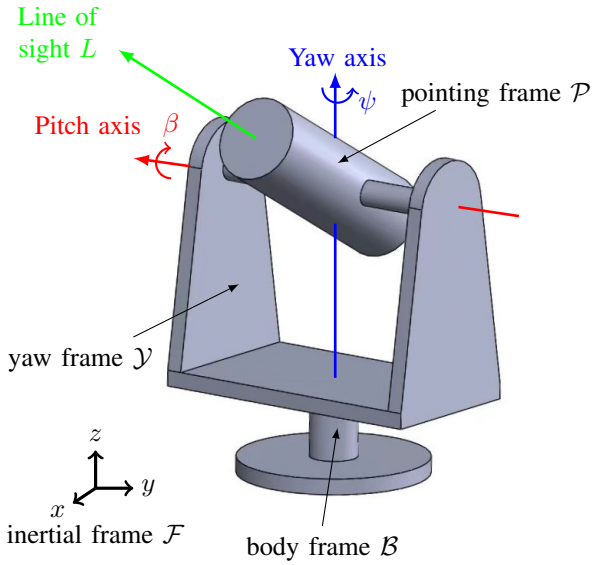

Fig. 1: The two-axis gimbal system coordinates and notations.

We have the following rotation matrix representation:

$$\mathbf{R}_{\mathcal{PY}}(\beta) = \begin{bmatrix} \cos\beta & 0 & \sin\beta \\ 0 & 1 & 0 \\ -\sin\beta & 0 & \cos\beta \end{bmatrix} \tag{1}$$

$$\mathbf{R}_{\mathcal{YB}}(\psi) = \begin{bmatrix} \cos\psi & -\sin\psi & 0 \\ \sin\psi & \cos\psi & 0 \\ 0 & 0 & 1 \end{bmatrix} \tag{2}$$

The task of the gimbal control system is to aim at a given direction, denoted by line-of-sight (LOS), which is a 3-dimensional real vector $L \in \mathbb{R}^3$ defined in inertial frame with $\|L\|_2 = 1$. The rotational matrices and desire line-of-sight satisfy

$$L(\psi, \beta) = \mathbf{R}_{\mathcal{PF}}(\psi, \beta) \cdot \mathbf{e}_1 \tag{3}$$

where $\mathbf{e}_1 \triangleq \begin{bmatrix} 1 & 0 & 0 \end{bmatrix}^\top$ is the canonical basis vector pointing to the direction of x-axis in the inertial frame. When $\psi = \beta = 0$, we have $\mathbf{R}_{\mathcal{PF}}(\psi, \beta) = I$ and $L(\psi, \beta) = \mathbf{e}_1$. We intend to solve desired yaw and pitch angle to accomplish the pointing task. Given the desired line-of-sight L^*, from equation (3) we have $\mathbf{R}_{\mathcal{YB}}(\psi) \cdot \mathbf{R}_{\mathcal{PY}}(\beta) \cdot \mathbf{e}_1 = \mathbf{R}_{\mathcal{BF}}^\top L^*$ which is equivalent to

$$\begin{bmatrix} \cos(\beta)\cos(\psi) \\ \cos(\beta)\sin(\psi) \\ -\sin(\beta) \end{bmatrix} = \mathbf{R}_{\mathcal{BF}}^\top L^* \tag{4}$$

One can obtain the desired β and ψ by solving (4). Denote them as β^*, ψ^*.

Given desired angles β^*, ψ^*, we intend to control the corresponding motor to track the desired angle.

B. System dynamics

We provide a kinetic model of the two-axis gimbal system for better understanding of the system before designing control algorithms. The system is composed of two parts. The motor system has inputs current of two motors i_β, i_ψ and outputs torques τ_β, τ_ψ. The rigid body kinetic system has input torques τ_β, τ_ψ and output angle β, ψ. We introduce their dynamics in the following.

1) Rigid body yaw kinetic: The pitch angle β has an influence on the dynamics of yaw system in two ways. Firstly, the tilted rigid body will change the mass moment of inertia (MMI) when tilt angle β changes. Secondly, there is an offset between the center-of-gravity (CoG) of the pointing system and the yaw axis, thus the distance of CoG and yaw axis will change by β, whice influences the MMI. We have the following kinetics on yaw angle.

$$\tau_\psi = I_\psi(\beta)\ddot{\psi} = \left[I_{\psi z}(\beta) + m_\psi(l_c\cos(\beta))^2\right]\ddot{\psi}, \tag{5}$$

where $I_{\psi z}(\beta)$ is the mass moment of inertia of the yaw rigid with respect to its center-of-gravity (CoG) and axis parallel to yaw axis. m_ψ is the mass of the yaw rigid. l_c is the length of CoG off-set along with the pointing axis (see Fig. 2).

$$I_{\psi z}(\beta) \triangleq I_{\psi yy} - (I_{\psi yy} - I_{\psi zz})\cos^2(\beta). \tag{6}$$

where $I_{\psi yy}$ and $I_{\psi zz}$ are mass moment of inertia of the yaw system about principal y-axis and principal z-axis, which can be measured accurately.

2) Rigid body pitch kinetic: For the pitching system, the rotation of yaw motor will provide extra inertial force on the pitch kinetics, due to the offset between the CoG of the pointing system and the yaw axis.

$$\tau_\beta - m_\beta\dot{\psi}^2 l_c\cos(\beta)\cdot l_c\sin(\beta) = \ddot{\beta}I_\beta \tag{7}$$

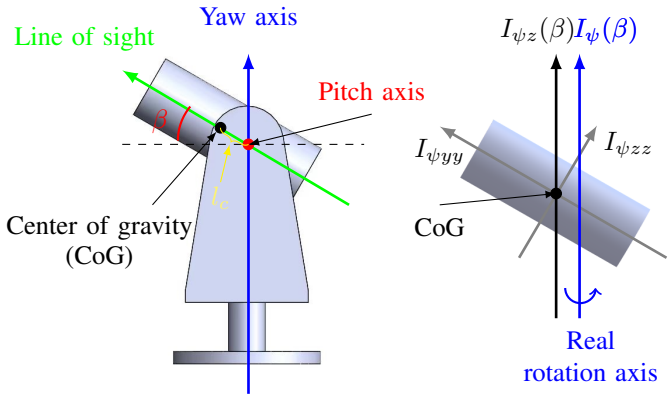

Fig. 2: The mass moment of inertia of a tilted rigid body.

where $m_\psi \dot{\psi}^2 l_c \cos(\beta)$ is the centrifugal force term and $l_c \sin(\beta)$ is the arm length of the force. m_β is the pitch system mass. I_β is the pitch MMI, and can be calculated by

$$I_\beta = I_{\beta xx} + m_\beta l_c^2. \tag{8}$$

3) Motor dynamics: Brushless DC (BLDC) motors are widely employed in various applications due to their remarkable characteristics. In particular, they find a pivotal role in various pointing systems [11], where precision and responsiveness are of paramount importance. One of the key advantages of BLDC motors is their high efficiency, which minimizes energy consumption and heat generation, crucial for delicate equipment like camera pointing systems or camera gimbal system. Additionally, BLDC motors offer precise control over position and velocity, making them an ideal choice for tracking moving targets with exceptional accuracy.

To harness the full potential of BLDC motors, advanced control strategies such as Field-Oriented Control (FOC) are employed. FOC allows for independent control of torque and flux components, enhancing motor performance and efficiency. FOC operates on the principle of decoupling the motor's stator currents into two components: the torque-producing current (i_d) and the magnetic field-aligning current (i_q). This decoupling is achieved by employing mathematical transformations that align the stator current vectors with the rotor's magnetic field orientation.

By independently controlling these two current components, FOC ensures precise management of motor behavior. The relationship between torque and current in BLDC motors is fundamental to their operation. It can be expressed by the equation:

$$\tau_\psi = \kappa_\psi i_\psi, \tau_\beta = \kappa_\beta i_\beta, \tag{9}$$

where τ is the torque generated by the motor and i is the current supplied to the motor. κ is the motor's torque constant. The dynamic relationship from current to torque for the motor is referred to the (forward) dynamics, while the relationship from torque to current is called the inverse dynamics. Thanks to the simple linear form in (9), the inverse dynamics is also linear and will be utilized in our control scheme.

Measuring or determining the motor's constants such as κ can be achieved through experimental testing, where torque and current are precisely measured under controlled conditions. Alternatively, manufacturers often provide these constants in motor specifications [12]. We assume the constant κ is known. We will introduce how to obtain such a value in simulation section (Section IV).

For the aforementioned analysis, we observe that the motors has decoupled dynamics for yaw and pitch axis, while the kinetics are coupled due to the shift of CoG from rotation axis and nature of grid body mechanics.

III. Gimbal Control System

In this section, we will introduce our proposed control algorithm framework to achieve stable and accurate control performance under camera-pointing task and gimbal-stabilizing task.

A. Overview of the Control Algorithm

The control algorithm is illustrated in 3. The system dynamics is in orange box, with motor dynamics decoupled between pitch and yaw axis, while the gimbal system has coupled dynamics, as shown in Section II. The observer is in green dashed box (introduced in Subsection III-C), with noisy measurement from encoders as the input and the filtered angle and angular velocity as output. Our control scheme is in the blue dashed box, mainly composed of double PID loops (introduced in Subsection III-B), feed-forward compensator in the red box (introduced in Subsection III-D) and motor inverse dynamics in the blue box (introduced in Subsection IV-B). The compensator aims at compensating the non-linear coupling terms in (5) to (8) and results in a decoupled double integrator ideal system:

$$\begin{cases} \tau_\psi = I_\psi^{\text{dec}} \cdot \ddot{\psi} \\ \tau_\beta = I_\beta^{\text{dec}} \cdot \ddot{\beta} \end{cases}, \tag{10}$$

where the superscript dec represents "decoupled". The value $I_\psi^{\text{dec}}, I_\beta^{\text{dec}}$ will be clear in Subsection III-D. However, since ψ, β is composed measurement noise and their time-derivative is not directed measured, we need an observer to estimate those states. The two double-loop integrator is designed to control the decoupled system (10) with fast response and precise tracking. Since the compensation is based on torques while our control input is the current, we need motor inverse dynamics to calculate the required current based on torque demand. We detail our design in the following subsections.

B. PID Control Algorithm

PID is a commonly used feedback control algorithm used to adjust the output of a system to approach a desired target value. Define the error of interested angles as

$$e_\psi = \psi - \psi_{\text{ref}}, \; e_\beta = \beta - \beta_{\text{ref}}, \tag{11}$$

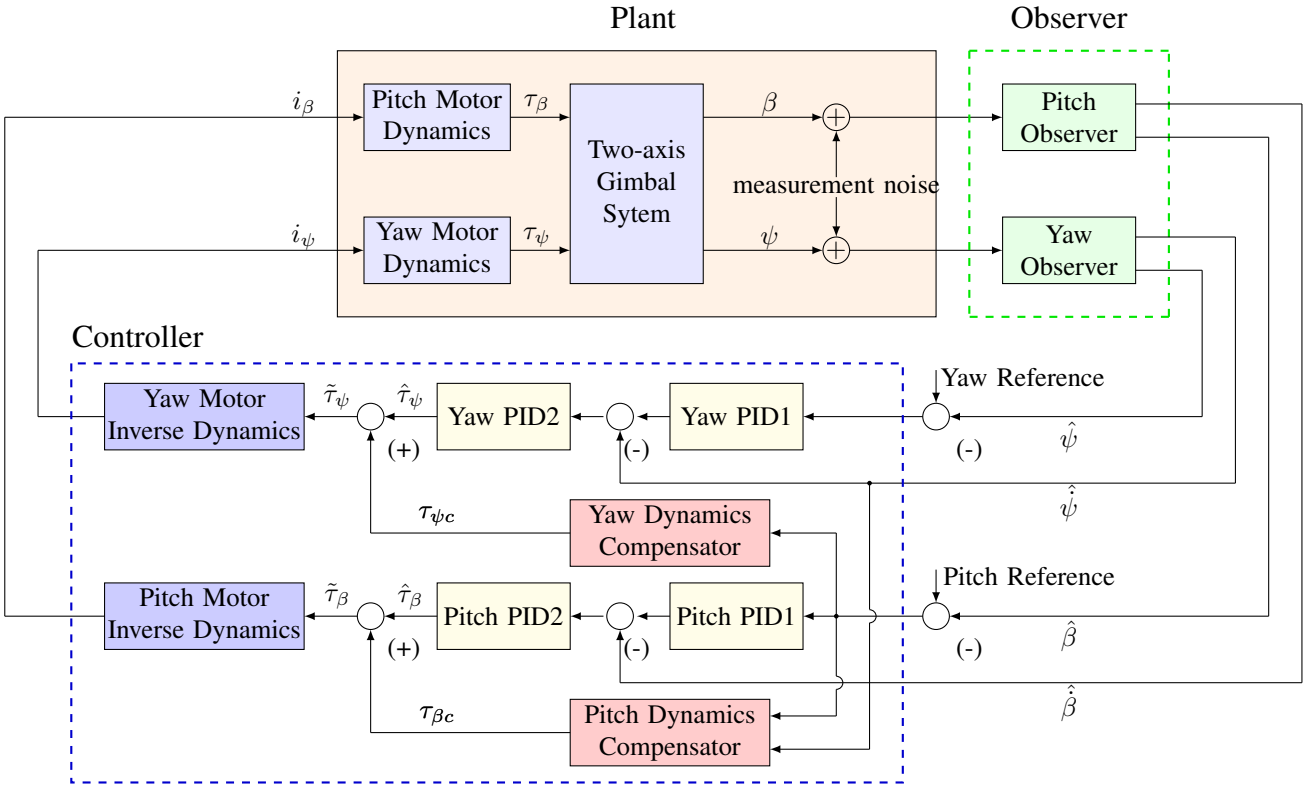

Fig. 3: Overview of the Control System.

where the subscript "ref" stands for reference signal. However, the control algorithm can only obtain the estimates states:

$$\hat{e}_\psi = \hat{\psi} - \psi_{\text{ref}}, \ \hat{e}_\beta = \hat{\beta} - \beta_{\text{ref}}. \tag{12}$$

The traditional PID controller calculates the control output based on the current error (the difference between the target value and the actual value), the integral of the error, and the rate of change of the error [13].

$$\hat{\tau}_\psi(t) = K_P^\psi \hat{e}_\psi(t) + K_I^\psi \int \hat{e}_\psi(t)\mathrm{d}t + K_D^\psi \cdot \hat{\dot{e}}_\psi(t), \tag{13}$$

$$\hat{\tau}_\beta(t) = K_P^\beta \hat{e}_\beta(t) + K_I^\beta \int \hat{e}_\beta(t)\mathrm{d}t + K_D^\beta \cdot \hat{\dot{e}}_\beta(t). \tag{14}$$

The PID we use in this paper is the PID controller with filter coefficient parameter N ,which can filter out high-frequency corrections to make K_D more useful:

$$\hat{\dot{e}}_i(s) = \frac{N}{1 + N\frac{1}{s}} \hat{e}_i(s), \ i \in \{\psi, \beta\}, \tag{15}$$

where s stands for the variable of Laplacian transformation.

We employ cascade PID control for the gimbal, consisting of a position loop (outer loop) and a velocity loop (inner loop). Compared to single-loop PID control, which only provides feedback of the system's attitude angle to the front end, cascade PID can be seen as state feedback, where both state variables are fed back to the front end of the controller. This enhances the gimbal's disturbance rejection capability and improves control quality. The PID cascade control structure of the gimbal is shown in Figure 2.

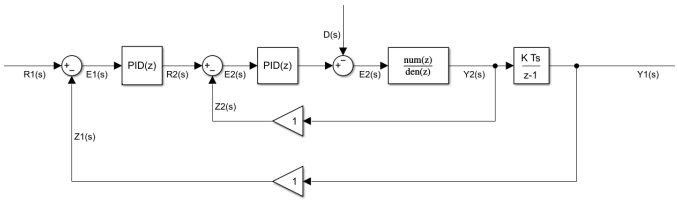

Fig. 4: General form of cascade PID system.

C. Luenberger observer

In order to obtain the accurate estimate of the noisy or unmeasurable angle states, we need to construct an observer for each angle. The system dynamics of the angle and angular velocity is model by the following linear time-invariant system:

$$\begin{cases} \dot{x} = Ax + Bu \\ y = Cx \end{cases}. \tag{16}$$

Among them, the state variable x, input variable u, output variable y, dynamic matrix A, and control matrix B, measure

matrix C are defined in the following from the decoupled ideal system (10):

$$x = \begin{bmatrix} \beta \\ \dot{\beta} \\ \psi \\ \dot{\psi} \end{bmatrix}, u = \begin{bmatrix} \tau_\beta \\ \tau_\psi \end{bmatrix}, y = \begin{bmatrix} \beta \\ \psi \end{bmatrix},$$

$$A = \mathrm{diag}\left(\begin{bmatrix} 0 & 1 \\ 0 & 0 \end{bmatrix}, \begin{bmatrix} 0 & 1 \\ 0 & 0 \end{bmatrix} \right),$$

$$B = \begin{bmatrix} 0 & 0 \\ \frac{1}{I_\beta^{\mathrm{dec}}} & 0 \\ 0 & 0 \\ 0 & \frac{1}{I_\psi^{\mathrm{dec}}} \end{bmatrix}, C = \begin{bmatrix} 1 & 0 & 0 & 0 \\ 0 & 0 & 1 & 0 \end{bmatrix}.$$

According to the known system, we establish an observer, and add output error feedback correction based on this. In which, L is the designed observer gain matrix.

$$\dot{\hat{x}} = A\hat{x} + Bu + L(y - C\hat{x}). \tag{17}$$

We have the following lemma claiming the stability of observer (17). The proof is trivial and thus omitted.

Lemma 1: For dynamic system in the form of (16), by choosing L such that $A - LC$ is Schur stable, the estimation error converges to zero:

$$\begin{bmatrix} \hat{\beta} \\ \dot{\hat{\beta}} \end{bmatrix} \to \begin{bmatrix} \beta \\ \dot{\beta} \end{bmatrix}, \begin{bmatrix} \hat{\psi} \\ \dot{\hat{\psi}} \end{bmatrix} \to \begin{bmatrix} \psi \\ \dot{\psi} \end{bmatrix}.$$

D. Feedforward compensation control design

Due to the physical structure of the system and the dynamic coupling analysis of the gimbal shown above, it can be seen that the influence between the yaw and pitch channels are non-linear and non-symmetric. To alleviate coupling effect and make full use the rich research results on the control of double-integrator system, we propose a feed-forward compensation mechanism in this subsection.

We reorganize the system mechanics from equation (5)-(8):

$$\tau_\psi = \underbrace{\left(m_\psi l_c^2 - I_{\psi yy} + I_{\psi zz}\right)\cos^2(\beta)\ddot{\psi}}_{\text{coupling term}} + I_{\psi yy}\ddot{\psi}. \tag{18}$$

$$\tau_\beta = \underbrace{m_\beta l_c^2 \cos(\beta)\sin(\beta)\dot{\psi}^2}_{\text{coupling term}} + \left(I_{\beta xx} + m_\beta l_c^2\right)\ddot{\beta}. \tag{19}$$

We split the angle accelerator term from other coupling terms and try to compensate these non-linear coupling terms by feed-forward.

We define $\tau_{\beta c}$ and $\tau_{\psi c}$ as the compensating torque of pitch axis and yaw axis respectively. And the compensator can only obtain the estimated angle and their time-derivatives, denoted by hat notations. The estimation of these states has been introduced in Subsection (III-C).

$$\tau_{\psi c} = \left(m_\psi l_c^2 - I_{\psi yy} + I_{\psi zz}\right)\cos^2(\hat{\beta})\ddot{\hat{\psi}}, \tag{20}$$

$$\tau_{\beta c} = m_\beta l_c^2 \cos(\hat{\beta})\sin(\hat{\beta})\dot{\hat{\psi}}^2. \tag{21}$$

Since the motor inverse dynamics may be slightly incompatible to real motor dynamics due to temperature change etc., we denote the real input torque as

$$\tau_\psi = \tilde{\tau}_\psi + d_\psi = \hat{\tau}_\psi + \tau_{\psi c} + d_\psi, \tag{22}$$

where d_ψ is the disturbance caused by motor model mismatch. Plug the $\tau_{\psi c}$ from (20) and $\tau_{\psi c}$ from the yaw dynamic (18) into equation (22), one obtains:

$$\hat{\tau}_\psi + d_\psi = I_{\psi yy}\ddot{\psi} + \left(m_\psi l_c^2 - I_{\psi yy} + I_{\psi zz}\right)\left(\cos^2(\beta)\ddot{\psi} - \cos^2(\hat{\beta})\ddot{\hat{\psi}}\right).$$

According to Lemma 1 we arrive at the following Theorem:

Theorem 2: According to our deign of compensators in (20)-(21), the cascade PID controller is actually controlling a disturbed double integrator of the form (10), i.e.,

$$\hat{\tau}_\psi \to I_{\psi yy}\ddot{\psi} - d_\psi, \tag{23}$$

$$\hat{\tau}_\beta \to \left(I_{\beta xx} + m_\beta l_c^2\right)\ddot{\psi} - d_\beta. \tag{24}$$

IV. Simulation

In the simulation stage, we set up the mechanical structure of the system, and accurately model and analyze the internal dynamic coupling.

In order to obtain the simulation results under the actual operating conditions, the data of each module in the simulation are the actual gimbal parameters, which enables us to improve the applicability of the simulation controller in the actual environment.

TABLE I: Parameters of Gimbal System

item	value
$l_c(\mathrm{cm})$	0.016
$m_\beta(\mathrm{kg})$	2.93
$m_\psi(\mathrm{kg})$	1.82
$I_{xx}(\mathrm{kg}\cdot\mathrm{m}^2)$	0.0829
$I_{yy}(\mathrm{kg}\cdot\mathrm{m}^2)$	0.0857
$I_{zz}(\mathrm{kg}\cdot\mathrm{m}^2)$	0.0794

For the gimbal control task, the two most important points are as follows: accurate tracking of the given target, the tracking and anti-disturbance ability of the head when the base is disturbed. So we give step and time-varying signals to the target in the simulation to demonstrate the superiority of our feedforward torque compensation in the gimbal control task.

In order to validate the control algorithm performance, we first show the estimation performance under measurement noise in Subsection IV-A. We further designed two reference signals to collaborate the control performance in real world applications, i.e., the step reference in Subsection IV-B and the time-varying reference in Subsection IV-C.

A. Observer effect

The raw measurement from sensors are usually corrupted by noises from real-world disturbance or measurement hardware. We simulate with measurement noise from the Band-Limited

White Noise module in simulink to better mimic the real-world scenarios. By comparing the angle value and angular velocity value estimation and raw noisy measurement, it can be found that the noise are filtered out with neglectable phase lag, which provides the control algorithm better feedback for accurate and timely response.

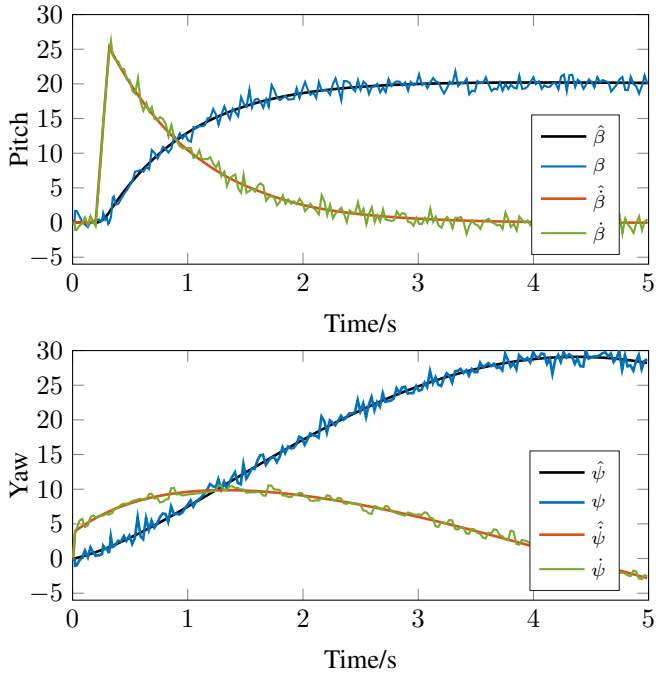

Fig. 5: Observation Effect of Gimbal.

B. Constant excitation

Given the fixed expected angle signals of pitch channel and yaw channel, the tracking capabilities of traditional PID control and dynamic torque compensation methods are compared by simulation. The results are shown in the following figures.

We demonstrate the PID parameters in yaw and pitch channels used in our simulation in Table II. We use same parameters in PID control and our proposed algorithm in the following figures to validate the performance improvement by dynamic feedforward compensation.

TABLE II: Response of the system

Channel	Response of the system			
	PID_Compensator		PID	
	t_s(s)	Overshoot (%)	t_s(s)	Overshoot (%)
Pitch	0.62	0.4	1.24	3
Yaw	0.66	0.4	1.54	1.95

Compared with the traditional PID control, our proposed dynamic feedforward compensated PID control method has smaller overshoot and faster convergence to the given reference under random disturbance, which collaborated the effectiveness of our proposed method.

From Fig. 7, one can see that the torque compensation exhibits similar response trends with the real torque demand,

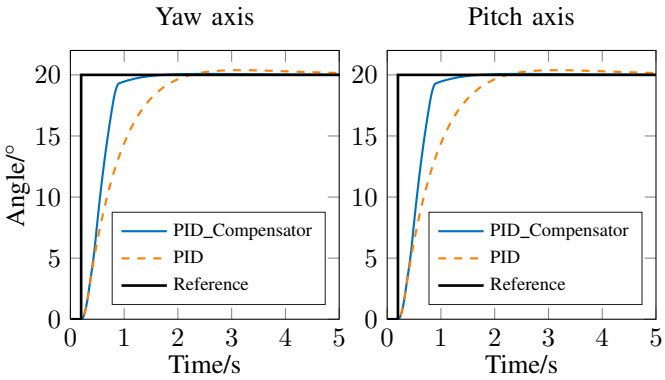

Fig. 6: Response of pitch and yaw angle under step signal reference. PID_Compensator represents our proposed dynamic feedforward compensated PID algorithm.

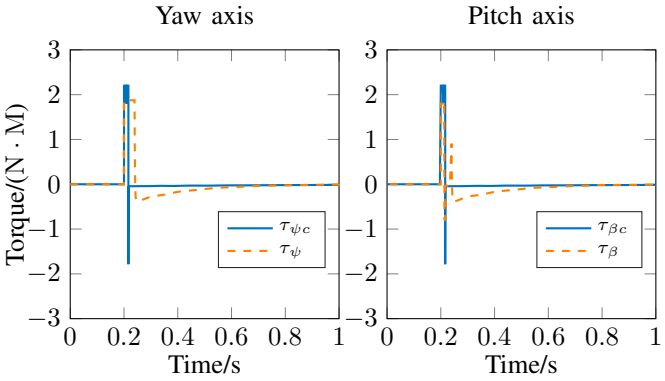

Fig. 7: Torque response of pitch and yaw angle under step signal reference. We only plot first 1 second since the torque basically converges to zero after it.

resulting less control effort by the PID controller and faster dynamic response.

C. Time-varying excitation

In this section, we give the system time-varying reference to verify the ability of the system to follow time-varying signals and the advantages of torque feedforward compensation under real-world tracking tasks. We give different time-varying signals to the pitch axis and yaw axis at the same time and observe their tracking performance in Fig. 8.

As seen from Fig. 8, the dynamic tracking error of our proposed algorithm (in blue line) is smaller than pure PID control, demonstrates superior performance in tracking dynamic reference angles, thus highlighting the promising application prospects of our algorithm.

V. Conclusion

In this paper, we propose a dynamic feedforward compensation control algorithm for the two-axis gimbal system. We first analyzed the mechanics of the two-axis system, and arrived at equations (5)-(8) describing the dynamic coupling of two axis due to tilted center-of-gravity (CoG) and varying

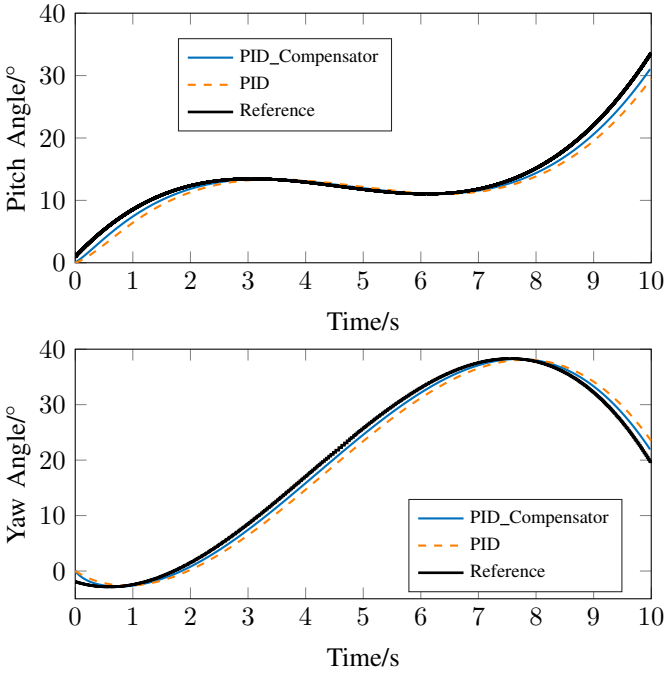

Fig. 8: Angle tracking performance of time-varying signal.

mass moment of inertia (MMI). In light of these challenges, we devised the dynamic feedforward compensation term to address the non-linear coupling, yielding an ideal double-integrator system, for which control algorithms have been extensively studied, making them easier to analysis. We further designed Luenberger observer to filter out noises and obtain signal time-derivatives for the usage of compensators and controllers. After compensation, the tracking error is handled by dual cascade PID controller. We have proved that the controller is essentially stabilizing a double-integrator system after compensation, which is promised to have better performance than direct stabilizing the original non-linear coupling system. Simulation results, underpinned by real-world parameter settings, validate our approach, showcasing its superiority in ensuring precise and agile control. This paper not only expands the theoretical landscape of gimbal control but also provides a practical framework for future innovations in the field.

REFERENCES

[1] Z. Yu, "A novel tandem ducted fan UAV attitude control based on cascade PID controller," in *2023 42nd Chinese Control Conference (CCC)*, 2023, pp. 4304–4310.

[2] H. Kang, H. Li, J. Zhang, X. Lu, and B. Benes, "Flycam: Multitouch gesture controlled drone gimbal photography," *IEEE Robotics and Automation Letters*, vol. 3, no. 4, pp. 3717–3724, 2018.

[3] R. J. Rajesh and P. Kavitha, "Camera gimbal stabilization using conventional PID controller and evolutionary algorithms," in *2015 International Conference on Computer, Communication and Control (IC4)*, 2015, pp. 1–6.

[4] A. R. Yasin, M. Ashraf, A. Plesca, S. Ahmad, R. Nasir-ullah, H. Naseer, and M. Adam, "Camera calibration and tracking for gimballed like eye structure in robots with hardware implementation," in *2017 International Conference on Electromechanical and Power Systems (SIELMEN)*, 2017, pp. 026–030.

[5] M. Řezáč and Z. Hurák, "Vibration rejection for inertially stabilized double gimbal platform using acceleration feedforward," in *2011 IEEE International Conference on Control Applications (CCA)*, 2011, pp. 363–368.

[6] Q. Mu, G. Liu, M. Zhong, and Z. Chu, "Imbalance torque compensation for three-axis inertially stabilized platform using acceleration feedforward," in *2012 8th IEEE International Symposium on Instrumentation and Control Technology (ISICT) Proceedings*, 2012, pp. 157–160.

[7] X. Han, W. Ma, J. Zhou, and C. Wang, "Accurate compensation of moving-gimbal effects in magnetically suspended control moment gyroscope," in *2021 36th Youth Academic Annual Conference of Chinese Association of Automation (YAC)*, 2021, pp. 125–128.

[8] S. Zheng, J. Xie, C. Ma, H. Liao, and C. Chen, "Improving dynamic response of amb systems in control moment gyros based on a modified integral feedforward method," *IEEE/ASME Transactions on Mechatronics*, vol. 22, no. 5, pp. 2111–2120, 2017.

[9] P. Cui and N. Yan, "Research on modeling of the agile satellite using a single gimbal magnetically suspended cmg and the disturbance feedforward compensation for rotors," *Sensors*, vol. 12, no. 12, pp. 16 964–16 987, 2012. [Online]. Available: https://www.mdpi.com/1424-8220/12/12/16964

[10] M. Özçelik, B. Kürkçü, and Z. Y. Bayraktaroğlu, "Modelling and simulation of 2 DOF gimbal system with experimental system identification," in *2022 10th International Conference on Systems and Control (ICSC)*, 2022, pp. 508–515.

[11] G. Özdoğan and K. Leblebicioğlu, "Cogging torque disturbance rejection for a low-cost gimbal motor and a controller design with practical considerations," in *2019 12th Asian Control Conference (ASCC)*, 2019, pp. 486–491.

[12] D.-J. Innovations. (2020) Robomaster gm6020 brushless dc motor user manual. [Online]. Available: www.robomaster.com

[13] M. A. Johnson and M. H. Moradi, *PID control*. Springer, 2005.